Article

Effect of Reactive Power Generation in Photovoltaic Installations on the Voltage Value at the Inverter Connection Point

Grzegorz Hołdyński [1], Zbigniew Skibko [1,*], Andrzej Borusiewicz [2,*], Andrzej Marczuk [3] and Adam Koniuszy [4]

1 Faculty of Electrical Engineering, Bialystok University of Technology, Wiejska 45D, 15-351 Bialystok, Poland
2 Department of Agronomy, Modern Technology and Informatics, International Academy of Applied Sciences in Lomza, 18-402 Lomza, Poland
3 Department of Agricultural, Forestry and Transport Machines, University of Life Sciences in Lublin, Głęboka 28, 20-612 Lublin, Poland
4 Department of Renewable Energy Engineering, West Pomeranian University of Technology in Szczecin, Pawla VI 1, 71-459 Szczecin, Poland
* Correspondence: z.skibko@pb.edu.pl (Z.S.); andrzej.borusiewicz@mans.edu.pl (A.B.)

Abstract: Worldwide, photovoltaic installations are making an increasing contribution to electric energy generation. These are power-unstable sources due to the rapid and frequent change in insolation. As a result, a common problem noted in low-voltage power grids is that the permitted voltage values at the source connection point are exceeded. There are several methods of limiting the voltage values present at the inverter. One of them is the generation of reactive power in a photovoltaic installation. In the literature, one can find many relationships that allow one to determine the increase in voltage caused by the change in reactive power, where the imaginary part of the voltage loss is omitted as insignificant. The authors' research has shown that this can lead to significant errors. Omitting the imaginary value causes the determined values to be even more than 4.5 times smaller—these differences increase with the length of the line. The analyses carried out by the authors show that the determination of voltage increments with and without taking into account the imaginary part of the voltage loss in the calculations differs from the values determined via computer simulation (failure to take into account the imaginary part results in calculated values of voltage increase being lower than the values determined via a computer by about 40% on average).

Keywords: voltage regulation; reactive power; power line; overvoltage

1. Introduction

As PV power generation capacity increases, its impact on the electric power system becomes greater [1,2]. The high variability of PV generation [3] causes difficulties during power system operation [4,5] and uncertainty in planning work [6]. Most of the energy generated by PV installations is produced during the circadian valley period, which is characterized by a significant reduction in system load, affecting the operation of conventional units [7]. Due to the randomness of the occurrence of solar energy in a given region, the amount of power generated in a PV installation varies over time. It significantly impacts the power quality delivered to consumers [8]. Therefore, it is recommended that PV power plants work with energy storage to increase the amount of self-consumption [9,10]. If this is not the case, it may lead to shutdowns of PV plants (e.g., resulting from exceeding the permissible voltage levels at the power plant's connection point) [11]. It can only be prevented by increasing the active participation of controlled load in regulating power system parameters [12].

The power generation of PV power plants above the demand of a given consumer causes an increase in voltage at their point of connection [13]. The operation of electrical installations at increased voltage levels reduces the insulation materials' strength (lifetime)

and, in extreme cases, can even lead to failure [14]. The voltage increase at the point of connection of PV installations depends on the power of the connected source and the structure of the grid [15]. A significant proportion of PV installations in a given area can significantly affect the stability of the power supply through outages caused by exceeding the acceptable voltage values. In addition, during disturbances in the power system, there are more significant voltage drops [16] and voltage oscillations in the lines, which can lead to voltage instability [17]. The magnitude of the disturbance introduced is mainly influenced by the power of the PV source, its location, and how the generated power is controlled [18]. More minor voltage fluctuations are noticed near the transformer station. PV systems equipped with three-phase inverters do not significantly affect the voltage imbalance that occurs on the grid [19]. However, installing multiple small PV systems with single-phase inverters significantly contributes to voltage unbalance [20]. The change in voltage at the connection point of a photovoltaic installation depends not only on the actual power generated but also on the system's impedance (which is influenced by the length and cross-section of the power line cables and the quality of the connections) [21]. No correlation has been observed between flicker factor values and the power generated in PV installations [22]. The effect of PV installations on voltage distortion—with prosumer installations—is negligible [23,24]. Exceedances of regulatory voltage distortion are mainly due to non-linear loads in the system [25,26].

The simplest and cheapest way to avoid unnecessary outages of PV installations resulting from an above-normal voltage value at the inverter connection point is to consume the power generated at the source by the consumers installed there [27]. When the load on the line is much smaller than the power generated by the PV installations, the voltage at any point on that power system is higher than the voltage at the feeder transformer. To prevent this, GFM inverters that mimic the behavior of synchronous generators can be used [28,29], or transformers can be replaced by autotransformers (however, this is a costly solution).

The regulation of voltage values can also be done from the inverter level. Seifi and Moallem showed that proportional-resonant controllers cannot accurately regulate the amplitude and phase of the current injected into the grid during frequency changes (resulting, for example, from PV plant operation). They proposed a synchronization method based on a closed-loop resonant filter derived from the internal model principle [30]. Implementing programmable control based on digital non-Foster electronics (using digital control techniques and switch electronics) avoids tedious manual operation, providing active circuits with real-time tuning [31].

As outlined in the introduction, the problem of voltage occurring at the point of connection of photovoltaic power plants is common and has been reported many times in the literature. One way to reduce the voltage at the inverter is to generate reactive power at the source. Although this issue is not new, some additional correlations not described in the literature were found as a result of the study carried out by the authors. This paper presents the results of a simulation study of the influence of parameters describing a given power system on the correlation between the amount of reactive power generated by the inverter and the voltage present at the connection point of the power plant.

2. Materials and Methods

In order to determine the influence of reactive power on the voltage value occurring in the power system, it is first necessary to determine the relationship that describes load-induced voltage changes. The complex value of the voltage loss in a power line caused by the flow of load power (active and reactive) can be described using the equation [32]:

$$\Delta \underline{U} = \frac{PR_k + QX_k}{U_{PCC}} + j\frac{PX_k - QR_k}{U_{PCC}} \qquad (1)$$

where P, Q is the active and reactive power of the line load, R_k, X_k is the equivalent resistance and reactance of the electric power network at the load or source switching point, U_{PCC} is the voltage at the load or source switching point.

The complex value of the unit voltage increase at the considered point of the network caused by the increase in the value of reactive power can be described as the derivative of the voltage loss relative to the reactive power:

$$\delta \underline{U}_0 = \frac{d(\Delta \underline{U})}{dQ} = \frac{X_k - jR_k}{U_{PCC}} = \frac{X_k}{U_{PCC}} - j\frac{R_k}{U_{PCC}} \quad \left[\frac{V}{var}\right] \tag{2}$$

For this case, the values of the absolute voltage increase can be expressed as follows:

$$\delta \underline{U} = \frac{X_k - jR_k}{U_{PCC}}\Delta Q = \frac{X_k}{U_{PCC}}\Delta Q - j\frac{R_k}{U_{PCC}}\Delta Q \quad [V] \tag{3}$$

where ΔQ is the increase in the value of reactive power.

It is commonly believed in the literature [32–34] that in the case of low-voltage transmission lines, the imaginary portion of the voltage loss is usually tiny and can be omitted. Therefore, the voltage drop is defined as the actual part of the voltage loss. Then, it can be written that the voltage increment at the grid point is equal to:

$$\delta U = \frac{X_k}{U_{PCC}}\Delta Q \tag{4}$$

Voltage drop can also be defined as the voltage loss modulus. It will then take the form of:

$$\delta U = \sqrt{\left(\frac{X_k}{U_{PCC}}\Delta Q\right)^2 + \left(\frac{R_k}{U_{PCC}}\Delta Q\right)^2} = \frac{\sqrt{R_k^2 + X_k^2}}{U_{PCC}}\Delta Q = \frac{Z_k}{U_{PCC}}\Delta Q \tag{5}$$

In order to verify the correctness of calculating the voltage changes determined using Relations (4) and (5), a computer model of a section of the power grid consisting of a 15/0.4 kV transformer station (with a 100 kVA transformer installed) and three low-voltage power lines of 2 km each was created. The overhead lines have 35, 50, and 70 mm² uninsulated conductors. Receiving and generating branches occur every 100 m. A schematic of this model is shown in Figure 1.
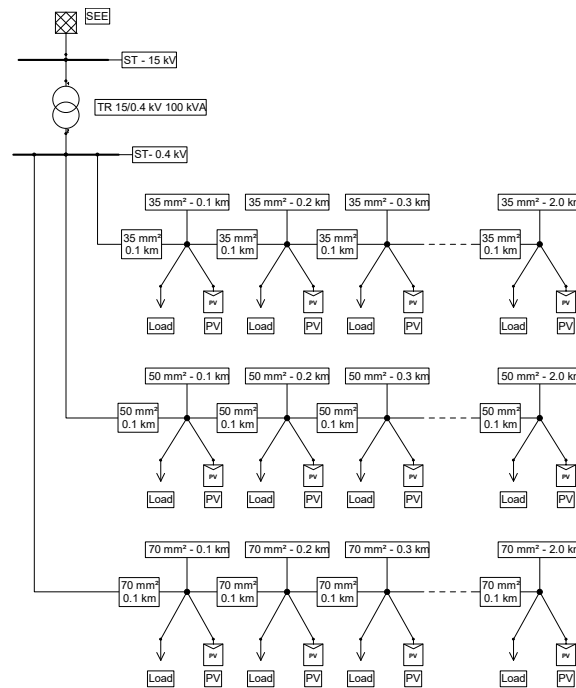

Figure 1. Diagram of the computer model of the electric power network under study.

The parameters of the power system section adopted for the analysis were as follows (Table 1).

Table 1. Parameters of the overhead lines.

Cross-Section	mm^2	35	50	70
resistance for positive component R1	Ω/km	0.836	0.592	0.417
reactance for positive component X1	Ω/km	0.336	0.325	0.313
capacitance for positive component C1	µF/km	0.010	0.011	0.011
resistance for zero component R0	Ω/km	1.262	0.991	0.763
reactance for zero component X0	Ω/km	1.316	1.192	1.083
current carrying capacity	A	175	220	275

Short-circuit parameters on the MV buses of the substation:

short-circuit power	100 MVA
short-circuit current	3.85 kA
short circuit impedance ratio (X_k/R_k)	2

Parameters of the MV/LV transformer supplying the low-voltage network:

rated power	100 kVA
rated overvoltage	15.75 kV
rated lower voltage	0.42 kV
connection group	Dyn5
short circuit voltage	4.5%
load loss	1.6 kW
idle losses	0.26 kW

Load parameters at individual network nodes:

active power	2 kW
reactive power	0.66 kvar
power factor cosφ	0.95

Generation parameters of PV installations connected to individual grid nodes:

active power	10 kW
reactive power	$-10 \div 10$ kvar

The low-voltage electric power network model created was subjected to voltage analysis using Neplan software (version 5.42). This software also allows the dynamic modelling and simulation of electric parameters in power systems with renewable energy sources.

The first stage of the analysis was to calculate the effect of reactive power generation on the voltage value using an analytical relationship (Relation (4)). It was followed by simulation calculations using the Neplan software. The final stage was to analyze and compare the results obtained.

Simulation calculations were carried out for individual PV power plant connection points. In the first case, the PV power plant generated no reactive power, while in the second case, a reactive power generation of 1 kvar of an inductive nature was assumed. In each case, the voltages at the connection point of the PV power plant were recorded, and then their difference was calculated, obtaining the voltage increment δU. Figures 2 and 3 show example simulation results in Neplan for the case of a PV power plant connection at a distance of 0.5 km from a substation.
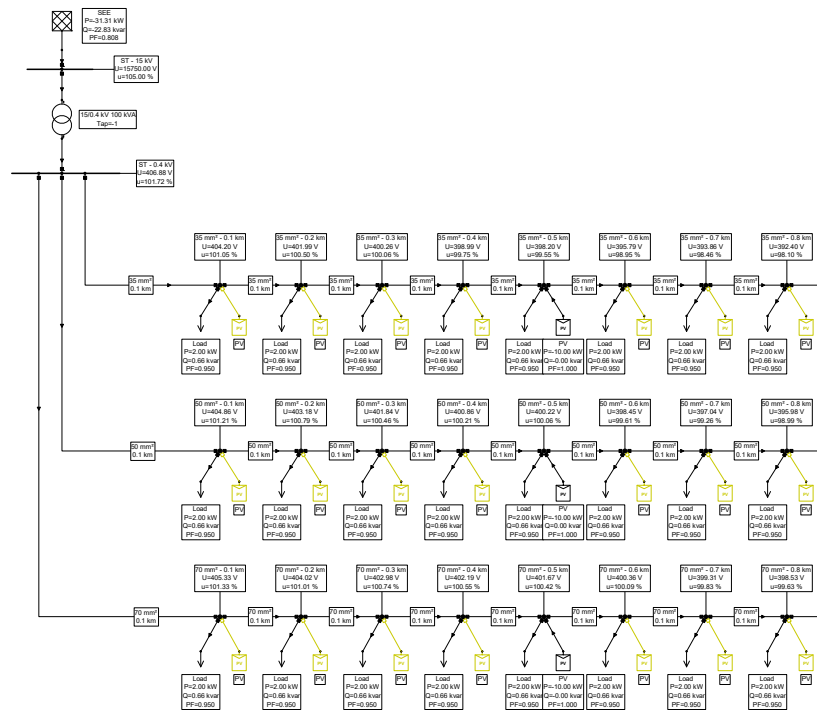
Figure 2. Example simulation results for power plants connected at a distance of 0.5 km from the substation without reactive power generation at the PV plant.
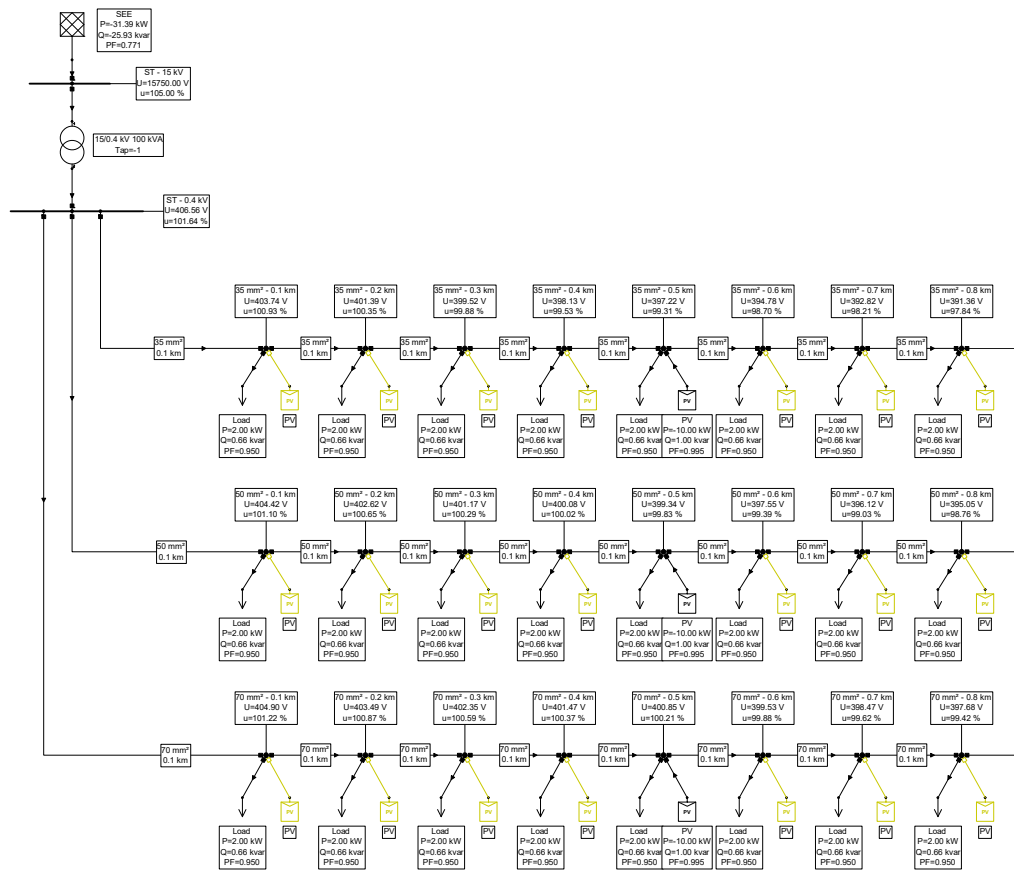

Figure 3. Example simulation results for power plants connected at a distance of 0.5 km from a substation with reactive power generation at a PV plant of 1 kvar.

In order to visualise the calculations and analyses carried out, a block diagram of the computer simulations and analytical calculations is shown in Figure 4.
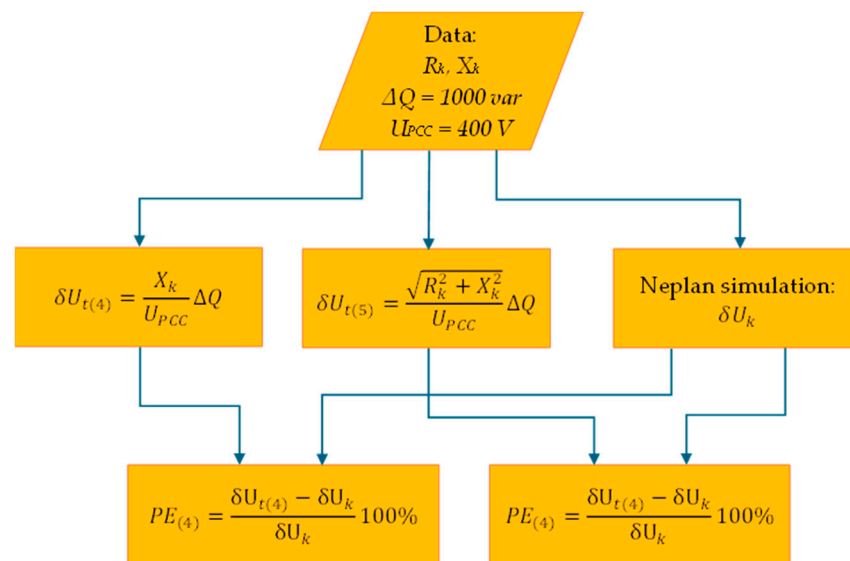

Figure 4. A block diagram of the simulations and analytical calculations was carried out.

3. Results and Discussion

For the same network parameters as those adopted in the computer model, the voltage gain (δU) was calculated using Relations (4) and (5). Results are shown in Figures 5 and 6.
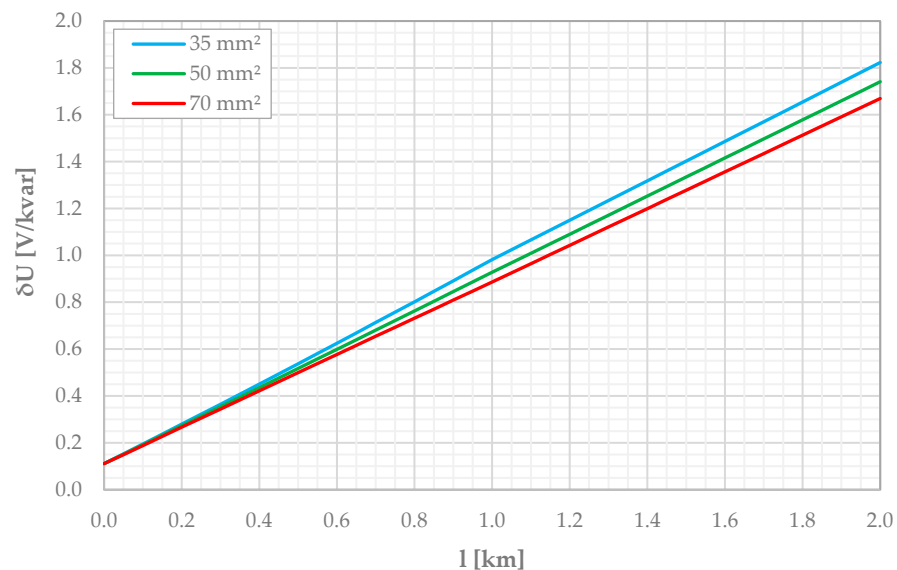

Figure 5. Voltage increment (δU) per 1 kvar of reactive power as a function of line length, determined according to Relation (4).

Analyzing the curves presented in Figure 5, it can be seen that the voltage increase caused by the change in reactive power increases linearly with the distance from the transformer station. With small line lengths (up to about 200 m), the cross-section of the line does not matter much. With the increase in the distance from the transformer station, the differences in the voltage increase for individual cross-sections increase, and the increase is more significant the smaller the cross-section of the line conductor.
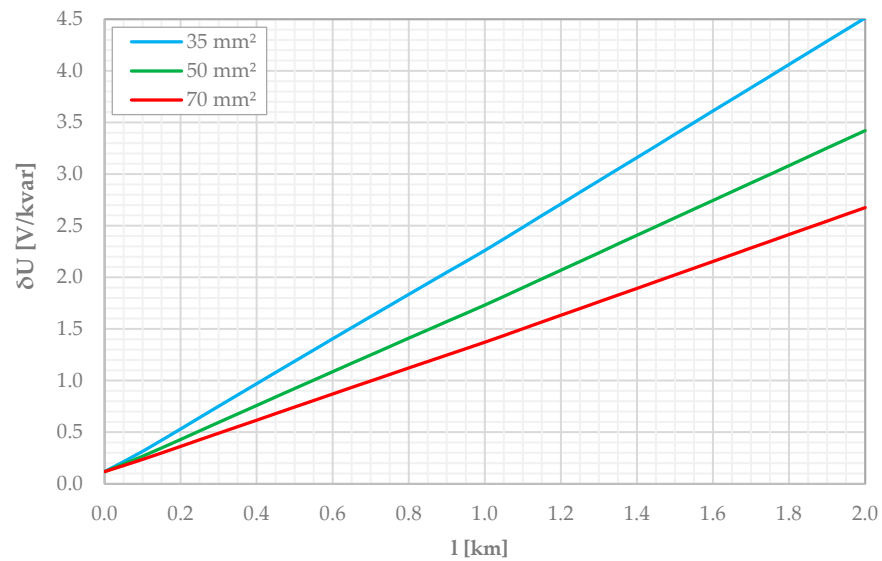
Figure 6. Voltage increment (δU) per 1 kvar of reactive power as a function of line length, determined according to the Relation (5).

Comparing the waveforms presented in Figures 5 and 6, it can be seen that the values of voltage increments caused by the change of reactive power determined from Relations (4) and (5) differ significantly. Considering the imaginary part in the calculations causes the voltage increments to differ significantly for different conductor cross-sections, practically in the entire analyzed line length range. This is because the resistance values are more significant in low-voltage power lines than the reactance. Table 2 shows the determined differences in the values of voltage increments determined from Relations (4) and (5). As can be seen, the values of voltage increment determined only from the natural part are even more than twice lower compared to the voltage increments determined from Relation (5). These differences decrease with the increase in the cross-section of wires in power lines.

Table 2. Results of theoretical calculations of voltage gain (δU).

Line Length	Voltage Increase (δU) Calculated via Relation (4) $\delta U_{t(4)}$			Voltage Increase (δU) Calculated via Relation (5) $\delta U_{t(5)}$			Ratio of Calculated Values $\delta U_{t(5)}/\delta U_{t(4)}$		
	35 mm²	50 mm²	70 mm²	35 mm²	50 mm²	70 mm²	35 mm²	50 mm²	70 mm²
[km]	[V/kvar]	[V/kvar]	[V/kvar]	[V/kvar]	[V/kvar]	[V/kvar]	[-]	[-]	[-]
0.0	0.111	0.111	0.111	0.118	0.118	0.118	1.06	1.06	1.06
0.1	0.195	0.192	0.189	0.315	0.268	0.237	1.61	1.40	1.26
0.2	0.280	0.273	0.267	0.532	0.430	0.363	1.90	1.58	1.36
0.3	0.365	0.355	0.345	0.752	0.595	0.490	2.06	1.68	1.42
0.4	0.451	0.436	0.422	0.970	0.759	0.617	2.15	1.74	1.46
0.5	0.538	0.518	0.500	1.188	0.923	0.744	2.21	1.78	1.49
0.6	0.625	0.599	0.577	1.405	1.086	0.871	2.25	1.81	1.51
0.7	0.714	0.681	0.655	1.621	1.249	0.997	2.27	1.83	1.52
0.8	0.802	0.763	0.732	1.836	1.411	1.123	2.29	1.85	1.53
0.9	0.892	0.846	0.809	2.049	1.572	1.248	2.30	1.86	1.54
1.0	0.982	0.928	0.887	2.261	1.733	1.372	2.30	1.87	1.55
1.1	1.066	1.009	0.965	2.486	1.901	1.503	2.33	1.88	1.56
1.2	1.150	1.091	1.043	2.711	2.070	1.633	2.36	1.90	1.57
1.3	1.234	1.172	1.122	2.937	2.239	1.763	2.38	1.91	1.57
1.4	1.318	1.253	1.200	3.161	2.408	1.894	2.40	1.92	1.58
1.5	1.403	1.335	1.278	3.387	2.576	2.024	2.41	1.93	1.58
1.6	1.487	1.416	1.357	3.613	2.745	2.154	2.43	1.94	1.59
1.7	1.571	1.497	1.435	3.836	2.914	2.285	2.44	1.95	1.59
1.8	1.655	1.579	1.513	4.062	3.082	2.415	2.45	1.95	1.60
1.9	1.739	1.660	1.592	4.288	3.253	2.546	2.47	1.96	1.60
2.0	1.823	1.741	1.670	4.512	3.421	2.676	2.48	1.97	1.60

In order to verify the curves shown in Figures 4 and 5, Figure 6 shows the dependence of voltage changes caused by the change in reactive power as a function of line length, determined based on computer simulation.

The lines of voltage increase caused by the change of reactive power shown in Figure 7 are not (compared to the values obtained analytically) straight-linear. In addition, these values are simultaneously more minor than the values determined from Relation (5) and more significant than the values calculated from Relation (4). In each analyzed case, however, the voltage increase decreases with the increase in the cross-section of the conductor used in the power line.
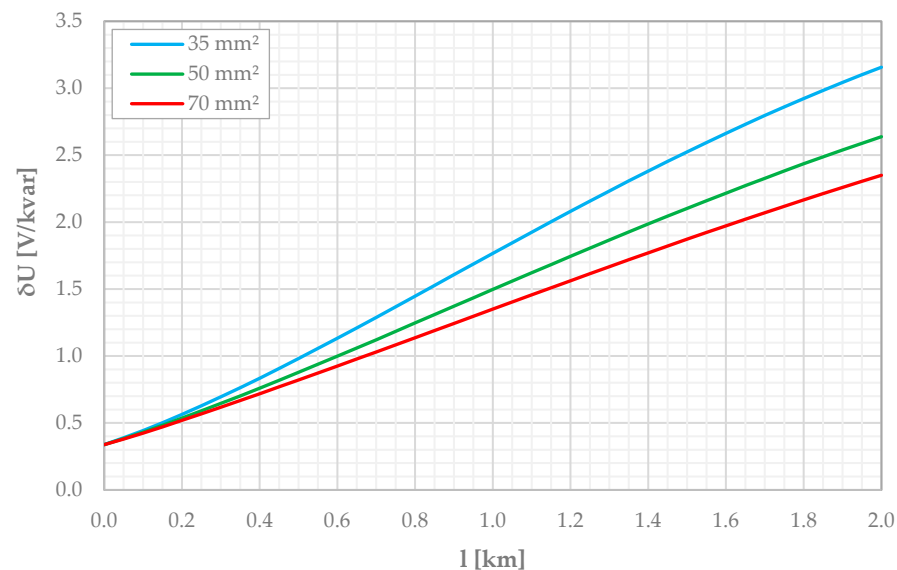

Figure 7. Voltage increment (δU) per 1 kvar of reactive power as a function of line length, determined based on computer simulation.

In addition, Table 3 presents the results of a comparative analysis of the values of voltage increments calculated theoretically and determined based on computer simulation. The following values of the percent error (PE) were used for the analysis:

$$PE = \frac{\delta U_t - \delta U_k}{\delta U_k} 100\% \tag{6}$$

where δU_t is the voltage increment per 1 kvar of reactive power calculated theoretically, δU_k—voltage increment per 1 kvar of reactive power calculated from computer simulation.

The analysis of the results presented in Table 3 shows that the failure to take into account the imaginary value (Relation (4)) when determining the voltage increase caused by the change in reactive power results in an average 40% underestimation of the obtained results in relation to the values obtained using the Neplan program. These differences decrease with the increase in distance from the transformer station and with the increase in the cross-sectional area of the conductor used to construct the line. Interesting relationships can be noticed by comparing the voltage increment determined from Relation (5) with the increase obtained in the computer simulation. In the vicinity of the transformer station, the voltage increments determined from Relation (5) are up to 60% smaller. For more considerable distances (depending on the cross-section of the line), the voltage increments determined in the Neplan program are greater than those determined in Relation (5). However, these differences are even several times smaller than in the case of using Relation (4).

Table 3. Results of a comparative analysis of the values of voltage increments calculated theoretically and determined based on computer simulation.

Line Length	Percentage Error of Voltage Increase Value Calculated via Relation (4) PE$_{(4)}$			Percentage Error of Voltage Increase Value Calculated via Relation (5) PE$_{(5)}$		
	35 mm²	50 mm²	70 mm²	35 mm²	50 mm²	70 mm²
[km]	[%]	[%]	[%]	[%]	[%]	[%]
0.0	−67.16	−67.16	−67.16	−65.12	−65.12	−65.12
0.1	−56.08	−55.56	−55.48	−29.08	−38.00	−44.08
0.2	−50.49	−49.16	−48.70	−5.77	−19.85	−30.19
0.3	−47.56	−45.21	−44.26	7.99	−8.05	−20.68
0.4	−45.99	−42.66	−41.31	16.22	−0.13	−14.15
0.5	−45.24	−41.13	−39.20	21.02	5.03	−9.46
0.6	−44.86	−40.08	−37.66	23.92	8.65	−5.96
0.7	−44.65	−39.28	−36.49	25.77	11.33	−3.29
0.8	−44.60	−38.84	−35.62	26.78	13.06	−1.26
0.9	−44.54	−38.37	−34.95	27.42	14.59	0.30
1.0	−44.43	−38.05	−34.38	27.96	15.67	1.59
1.1	−44.62	−37.78	−33.79	29.15	17.23	3.14
1.2	−44.73	−37.51	−33.25	30.28	18.63	4.49
1.3	−44.73	−37.24	−32.76	31.52	19.92	5.72
1.4	−44.66	−36.93	−32.26	32.68	21.17	6.93
1.5	−44.46	−36.54	−31.75	34.12	22.51	8.07
1.6	−44.20	−36.14	−31.25	35.60	23.83	9.20
1.7	−43.84	−35.69	−30.72	37.16	25.17	10.32
1.8	−43.39	−35.20	−30.15	38.98	26.53	11.50
1.9	−42.87	−34.63	−29.58	40.88	28.11	12.64
2.0	−42.27	−34.03	−28.98	42.88	29.64	13.82

Based on the results of computer simulations, empirical relationships were developed to calculate the value of the voltage gain (δU) caused by the change in reactive power. To determine the empirical relationships, STATISTICA (the calculations were performed using STATISTICA version 13.3 software, originally developed by StatSoft and now maintained by TIBCO Software Inc., Palo Alto, CA, USA) software was used using the method of polynomial regression approximated with a 3rd degree polynomial depending on the length of the line (l). Due to significant differences, separate equations have been developed for lines with different wire cross-sections:

- for 35 mm² cross-sectional line

$$\delta U_{35mm} = -0.1781l^3 + 0.5121l^2 + 1.0982l + 0.3301 \tag{7}$$

- for 50 mm² cross-sectional line

$$\delta U_{50mm} = -0.0983l^3 + 0.2839l^2 + 0.9765l + 0.3332 \tag{8}$$

- for 70 mm² cross-sectional line

$$\delta U_{70mm} = -0.0592l^3 + 0.1695l^2 + 0.9053l + 0.3342 \tag{9}$$

For all relationships, the value of the fit factor of the regression equation was $R^2 = 1$. It can also, at the expense of reducing the accuracy of the fit, simplify these relationships to linear equations:

- for 35 mm² cross-sectional line

$$\delta U_{35mm} = 1.471l + 0.2832 \tag{10}$$

- for 50 mm² cross-sectional line

$$\delta U_{35mm} = 1.1847l + 0.3065 \tag{11}$$

- for 70 mm^2 cross-sectional line

$$\delta U_{35\text{mm}} = 1.0276l + 0.3192 \tag{12}$$

The values of the fit factors of the regression equations are R^2 = 0.9987 for Equation (10), R^2 = 0.9994 for Relation (11), and R^2 = 0.9997 for Relation (12), respectively, which is considered to be sufficient accuracy.

Changing the voltage value in power grids by altering the reactive power generation has been proposed by Fukushima et al. [35,36], among others. Their proposed method shares information with all consumers in a low-voltage distribution line and autonomously injects reactive power according to a point. However, as the authors emphasized, this method was developed under laboratory conditions and must be verified on a real distribution network. A similar algorithm was used by Zhang et al. [33]. However, they, too, did not consider the dependence of voltage changes as a function R and X. Also, Moondee and Srirattanawichaikul [34] showed a theoretical relationship between voltage and the amount of reactive power generated. Bletterie et al. [37] propose a power control strategy based on the voltage and line impedance magnitude at the grid connection point, which uses the residual power of the inverter when the voltage at the grid connection point exceeds the upper limit. Ruiz-Tipán et al. [38] proposed using reactive power compensation, which is connected in parallel to the load, for voltage control. This paper, as well as in [39], highlighted the voltage instability that occurs with parallel compensation. According to the authors' analyses, this may be the reason for not considering the voltage dependence on the reactance-to-resistance ratio of the supply line. The use of a simple voltage regulation method has the problem of insufficient advantages and apparent disadvantages, which in most cases is insufficient to meet the requirements of a high penetration rate of distributed PV grid connection [40]. Zhang et al. [41] proposed a coordinated method for managing the reactive power margin of multiple PV inverters for voltage regulation. Based on the distribution network model, a relationship between the PV reactive power margin and the power flow was obtained. However, the analysis was carried out for the one line impedance value, not considering (as the authors of this article) the variation of the line impedance with its length.

4. Conclusions

The stabilization of the voltage at the point of connection of photovoltaic power plants is essential. Many researchers have dealt with this topic, paying particular attention to the possibility of regulating the voltage value at the connection point of the power plant by changing the reactive power flows. The relationships describing this phenomenon are not new and are repeatedly cited in various publications. As the authors have shown in this article, changing the voltage value dependent only on the actual equivalent impedance of the power supply system and the voltage occurring in the network can lead to significant errors. Other researchers realized this problem by stating that reactive power values calculated analytically could not be used to stabilize voltage values, and they based their proposed algorithms on direct measurements of quantities occurring in power grids. However, none of them attempted to find the source of this problem. Failure to consider the imaginary component when determining the voltage increase due to changes in reactive power leads to an average underestimation of approximately 40% compared to the results obtained from computer simulations. Calculating voltage changes taking into account the impedance of the circuit leads to more minor errors, but for short distances from the transformer station, these errors are harmful, as this only changes the sign and increases the value with the distance.

The relationships determined by the authors, showing the increase in voltage caused by the change of reactive power as a function of line length, are different for different cross-sections of power lines. Further work by the authors will continue towards the development of universal dependencies covering the type and cross-section of line wires and the type and power of the MV/LV transformer.

References

1. Achilles, S.; Schramm, S.; Bebic, J. *Transmission System Performance Analysis for High-Penetration Photovoltaics*; National Renewable Energy Laboratory (NREL): Golden, CO, USA, 2011. [CrossRef]
2. Chang, X.; Zhang, M.; Gao, L.; Mao, R.; Li, S.; Ma, N. An Analysis Method of the Influence of Distributed PV Location on Voltage and Harmonic Distribution of the Distribution Network. In Proceedings of the 2020 10th International Conference on Power and Energy Systems (ICPES), Chengdu, China, 25–27 December 2020; pp. 104–108. [CrossRef]
3. Chen, J.; Hu, H. Techno-Economic Model-Based Capacity Design Approach for Railway Power Conditioner-Based Energy Storage System. *IEEE Trans. Ind. Electron.* **2022**, *69*, 4730–4741. [CrossRef]
4. Stoyanov, I.; Iliev, T. Harmonic Distortion by Single-Phase Photovoltaic Inverter. In Proceedings of the 2019 11th International Symposium on Advanced Topics in Electrical Engineering (ATEE), Bucharest, Romania, 28–30 March 2019. [CrossRef]
5. Vadlamudi, B.; Anuradha, T. Review of islanding detection using advanced signal processing techniques. *Electr. Eng.* **2023**, *106*, 181–202. [CrossRef]
6. Madaeni, S.H.; Sioshansi, R.; Denholm, P. Comparing capacity value estimation techniques for photovoltaic solar power. *IEEE Trans. Photovolt.* **2014**, *3*, 407–415. [CrossRef]
7. Fischer, D.; Surmann, A.; Lindberg, K.B. Impact of emerging technologies on the electricity load profile of residential areas. *Energy Build.* **2019**, *208*, 109614. [CrossRef]
8. Rehman, W.; Bo, R.; Mehdipourpicha, H.; Kimball, J.W. Sizing battery energy storage and PV system in an extreme fast charging station considering uncertainties and battery degradation. *Appl. Energy* **2022**, *313*, 118745. [CrossRef]
9. Chen, Q.; Zhu, B.; Liu, M.; Mao, S. Analysis of Grid-Connected Stability of VSG-Controlled PV Plant Integrated with Energy Storage System and Optimization of Control Parameters. *Electronics* **2024**, *13*, 1343. [CrossRef]
10. Fumin, Z.; Song, B.A.I.; Zhankai, L.I. Control Strategy for Microgrid Storage System's State of Charge Based on Virtual Synchronous Generator. *Power Syst. Technol.* **2019**, *43*, 2109–2116. [CrossRef]
11. Shin, H.; Roh, J.H. Framework for Sizing Energy Storage System Supplementing Photovoltaic Generation in Consideration of Battery Degradation. *IEEE Access* **2020**, *8*, 60246–60258. [CrossRef]
12. Lu, S.; Diao, R.; Samaan, N.; Etingov, P. *Capacity, Value of PV and Wind Generation in the NV Energy System*; PNNL-22117; U.S. Department of Energy: Washington, DC, USA, 2012.
13. Alshamrani, A.; Majumder, P.; Das, A.; Hezam, I.M.; Božanić, D. An Integrated BWM-TOPSIS-I Approach to Determine the Ranking of Alternatives and Application of Sustainability Analysis of Renewable Energy. *Axioms* **2023**, *12*, 159. [CrossRef]
14. Gonzalez, P.; Romero-Cadaval, E.; Gonzalez, E.; Guerrero, M.A. Impact of grid-connected photovoltaic system in the power quality of a distribution network. In *Technological Innovation for Sustainability, Proceedings of the Second IFIP WG 5.5/SOCOLNET Doctoral Conference on Computing, Electrical and Industrial Systems, DoCEIS 2011, Costa de Caparica, Portugal, 22–24 February 2011*; Springer: Berlin/Heidelberg, Germany, 2011; pp. 466–473. [CrossRef]
15. Ma, C.; Xiong, W.; Tang, Z.; Li, Z.; Xiong, Y.; Wang, Q. Distributed MPC-Based Voltage Control for Active Distribution Networks Considering Uncertainty of Distributed Energy Resources. *Electronics* **2024**, *13*, 2748. [CrossRef]
16. Eftekharnejad, S.; Vittal, V.; Heydt, G.T.; Keel, B.; Loehr, J. 'Impact of increased penetration of photovoltaic generation on power systems. *IEEE Trans. Power Syst.* **2013**, *28*, 893–901. [CrossRef]
17. Holdyński, G.; Skibko, Z.; Firlit, A.; Walendziuk, W. Analysis of the Impact of a Photovoltaic Farm on Selected Parameters of Power Quality in a Medium-Voltage Power Grid. *Energies* **2024**, *17*, 623. [CrossRef]
18. Uddin, M.; Rahman, M.; Hossain, T.R.; Rahman, H. Assessment by Simulation of Different Topological Integration of Solar Photovoltaic Plants in Medium Voltage Distribution Networks. *Pertanika J. Sci. Technol.* **2021**, *29*, 1159–1169. [CrossRef]
19. Hołdyński, G.; Skibko, Z.; Firlit, A.; Borusiewicz, A. Analysis of the effect of symmetrical load on the value of negative voltage asymmetry factor in medium-voltage power networks. *Przegląd Elektrotechniczny* **2024**, 289–294. [CrossRef]
20. Holdyński, G.; Skibko, Z.; Borusiewicz, A. Analysis of the Influence of Load on the Value of Zero-Voltage Asymmetry in Medium-Voltage Networks Operating with Renewable Energy Sources. *Energies* **2023**, *16*, 580. [CrossRef]

21. Alam, S.; Al-Ismail, F.S.; Salem, A.; Abido, M.A. High-Level Penetration of Renewable Energy Sources Into Grid Utility: Challenges and Solutions. *IEEE Access* **2020**, *8*, 190277–190299. [CrossRef]

22. Wang, Y. Application of Solar Noise Barrier Power Generation System Envisaged on Urban Elevated Roads. *J. Phys. Conf. Ser.* **2020**, *1549*, 052118. [CrossRef]

23. Ghaffari, A.; Askarzadeh, A.; Fadaeinedjad, R.; Siano, P. Mitigation of total harmonic distortion and flicker emission in the presence of harmonic loads by optimal siting and sizing of wind turbines and energy storage systems. *J. Energy Storage* **2024**, *86 Pt B*, 111312. [CrossRef]

24. Li, F.; Xi, W.; Dai, X. 3D Modeling Technology Based on Computer Aided Environment Design. *J. Phys. Conf. Ser.* **2022**, *2146*, 012031. [CrossRef]

25. Deng, Z.; Rotaru, M.D.; Sykulski, J.K. Harmonic Analysis of LV distribution networks with high PV penetration. In Proceedings of the 2017 International Conference on Modern Power Systems (MPS), Cluj-Napoca, Romania, 6–9 June 2017; pp. 1–6. [CrossRef]

26. Penangsang, O.; Seto Wibowo, R.; Ketut Aryani, N.; Dwi Prasetyo, M.; Nicky Arianto, M.; Amjad Lutfi, A. Harmonic assessment on two photovoltaic inverter modes and mathematical models on low voltage network power quality. *Int. J. Electr. Comput. Eng. (IJECE)* **2023**, *13*, 5951–5965. [CrossRef]

27. Baier, C.R.; Melin, P.E.; Torres, M.A.; Ramirez, R.O.; Muñoz, C.; Quinteros, A. Developing and Evaluating the Operating Region of a Grid-Connected Current Source Inverter from Its Mathematical Model. *Mathematics* **2024**, *12*, 1775. [CrossRef]

28. Peng, F.Z.; Liu, C.C.; Li, Y.; Jain, A.K.; Vinnikov, D. Envisioning the Future Renewable and Resilient Energy Grids—A Power Grid Revolution Enabled by Renewables, Energy Storage, and Energy Electronics. *IEEE J. Emerg. Sel. Top. Ind. Electron.* **2024**, *5*, 8–26. [CrossRef]

29. Strunz, K.; Almunem, K.; Wulkow, C.; Kuschke, M.; Valescudero, M.; Guillaud, X. Enabling 100% Renewable Power Systems Through Power Electronic Grid-Forming Converter and Control: System Integration for Security, Stability, and Application to Europe. *Proc. IEEE* **2023**, *111*, 891–915. [CrossRef]

30. Seifi, K.; Moallem, M. An Adaptive PR Controller for Synchronizing Grid-Connected Inverters. *IEEE Trans. Ind. Electron.* **2019**, *66*, 2034–2043. [CrossRef]

31. Yang, X.; Zhang, Z.; Xu, M.; Li, S.; Zhang, Y.; Zhu, X.F.; Ouyang, X.; Alù, A. Digital non-Foster-inspired electronics for broadband impedance matching. *Nat. Commun.* **2024**, *15*, 4346. [CrossRef]

32. Lubośny, Z. Wind Turbine Operation in Electric Power System. In *Advanced Modelling*; Springer: Berlin, Germany, 2003; ISBN 978-3-642-07317-5. [CrossRef]

33. Zhang, F.; Guo, X.; Chang, X.; Fan, G.; Chen, L.; Wang, Q.; Tang, Y.; Dai, J. The reactive power voltage control strategy of PV systems in low-voltage string lines. In Proceedings of the 2017 IEEE Manchester PowerTech, Manchester, UK, 18–22 June 2017; pp. 1–6. [CrossRef]

34. Moondee, W.; Srirattanawichaikul, W. Study of Coordinated Reactive Power Control for Distribution Grid Voltage Regulation with Photovoltaic Systems. In Proceedings of the 2019 IEEE PES GTD Grand International Conference and Exposition Asia (GTD Asia), Bangkok, Thailand, 19–23 March 2019; pp. 136–141. [CrossRef]

35. Fukushima, K.; Nayuki, T.; Hatta, H.; Kobayashi, H. Voltage Regulation in Low-Voltage Distribution Grids with Reactive Power Control by Power Conditioning Subsystem Coordination. In Proceedings of the 2019 International Conference on Smart Energy Systems and Technologies (SEST), Porto, Portugal, 9–11 September 2019; pp. 1–5. [CrossRef]

36. Hu, Y.; Liu, W.; Wang, W. A Two-layer Volt-var Control Method in Rural Distribution Networks Considering Utilization of Photovoltaic Power. *IEEE Access* **2020**, *8*, 118417–118425. [CrossRef]

37. Bletterie, B.; Kadam, S.; Bolgaryn, R.; Zegers, A. Voltage Control with PV Inverters in Low Voltage Networks—In Depth Analysis of Different Concepts and Parameterization Criteria. *IEEE Trans. Power Syst.* **2017**, *32*, 177–185. [CrossRef]

38. Ruiz-Tipán, F.; Barrera-Singaña, C.; Valenzuela, A. Reactive Power Compensation Using Power Flow Sensitivity Analysis and QV Curves. In Proceedings of the 2020 IEEE ANDESCON, Quito, Ecuador, 13–16 October 2020; pp. 1–6. [CrossRef]

39. Ćetković, D.; Žutolija, J.; Komen, V. Voltage Rise Mitigation in Medium-Voltage Networks with Long Underground Cables and Low Power Demand. *Energies* **2024**, *17*, 3174. [CrossRef]

40. Gao, X.; Zhang, J.; Sun, H.; Liang, Y.; Wei, L.; Yan, C.; Xie, Y. A Review of Voltage Control Studies on Low Voltage Distribution Networks Containing High Penetration Distributed Photovoltaics. *Energies* **2024**, *17*, 3058. [CrossRef]

41. Zhang, Y.; Yi, H.; Zhang, H.; Wang, Q.; Yang, Z.; Zhuo, F. Coordinated Reactive Power Margin Management of Multiple Photovoltaic Inverters for Voltage Regulation in Distribution Networks. In Proceedings of the 2022 IEEE International Power Electronics and Application Conference and Exposition (PEAC), Guangzhou, Guangdong, China, 4–7 November 2022; pp. 1598–1602. [CrossRef]